REPORT DOCUMENTATION PAGE

Form Approved
OMB No. 0704-0188

PLEASE DO NOT RETURN YOUR FORM TO THE ABOVE ADDRESS.

1. REPORT DATE *(DD-MM-YYYY)*	2. REPORT TYPE	3. DATES COVERED *(From - To)*
20-12-2010	Final Performance Report	01 March, 2008 -- 30 November, 2010

4. TITLE AND SUBTITLE

Sensitive Infrared Photodetectors:
Optimized Electron Kinetics for Room-Temperature Operation

5a. CONTRACT NUMBER

FA9550-08-1-0127

5b. GRANT NUMBER

5c. PROGRAM ELEMENT NUMBER

6. AUTHOR(S)

Prof. Vladimir Mitin (PI),
Prof. Andrei Sergeyev (Co-I)

5d. PROJECT NUMBER

5e. TASK NUMBER

5f. WORK UNIT NUMBER

7. PERFORMING ORGANIZATION NAME(S) AND ADDRESS(ES)

The Research Foundation of SUNY
Sponsored Projects Services,
Suite 211, The UB Commons, 520 Lee Entrance, Amherst, NY 14228

8. PERFORMING ORGANIZATION REPORT NUMBER

9. SPONSORING/MONITORING AGENCY NAME(S) AND ADDRESS(ES)

RESEARCH FOUNDATION OF STATE
UNIVERSITY OF NEW YORK, THE
SPONSORED PROGRAMS ADM
402 CROFTS HALL
AMHERST NY 14260-0001

10. SPONSOR/MONITOR'S ACRONYM(S)

11. SPONSOR/MONITOR'S REPORT NUMBER(S)

AFRL-OSR-VA-TR-2012-0236

12. DISTRIBUTION/AVAILABILITY STATEMENT

A

13. SUPPLEMENTARY NOTES

14. ABSTRACT

The research focused on design of room-temperature detectors based on advanced quantum dot (QD) nanostructures with optimized photoelectron kinetics. It has been demonstrated that potential barriers around QDs and/or QD clusters significantly increase the photoelectron lifetime and improve the device responsivity, photoconductive gain, and sensitivity. Combining QD nanoblocks with various positions of dopants it is possible to create unique distribution of potential profile, which forces photoelectrons to move in the designated areas and to avoid QDs. Changing the electron occupation of QDs one can manage the barriers and control the photoelectron motion. The proposed, designed, and investigated advanced QD structures have a set of characteristics making them especially suitable for IR: (i) Manageable kinetics, which allows for tuning the photocarrier lifetime to control basic sensor characteristics, such as operating time, responsivity, and detectivity; (ii) Tunable highly-selective coupling to radiation; (iii) High photoconductive gain and responsivity; (iv) Low generation-recombination noise due to the long photoelectron lifetime.

15. SUBJECT TERMS

Infrared Photodetectors, Quantum Dot Structures

16. SECURITY CLASSIFICATION OF:			17. LIMITATION OF ABSTRACT	18. NUMBER OF PAGES	19a. NAME OF RESPONSIBLE PERSON
a. REPORT	b. ABSTRACT	c. THIS PAGE			Vladimir Mitin
U	U	U	UU	16	19b. TELEPHONE NUMBER *(Include area code)* 716-645-1036

Reset

Standard Form 298 (Rev. 8/98)
Prescribed by ANSI Std. Z39.18

AFOSR Final Performance Report

FA9550-08-1-0127

Sensitive Infrared Photodetectors: Optimized Electron Kinetics for Room Temperature Operation

Abstract:

This research focused on design of room-temperature detectors based on advanced quantum dot (QD) nanostructures with optimized kinetics of photoelectrons. It has been demonstrated that potential barriers around QDs and/or QD clusters significantly increase the photoelectron lifetime (the capture time of photoelectrons) and improve the device responsivity, photoconductive gain, and sensitivity. Combining QD nanoblocks with various positions of dopants it is possible to create unique distribution of potential profile, which forces photoelectrons to move in the designated areas with the lower potential and to avoid dots. Moreover, changing the electron occupation of quantum dots one can manage the potential barriers around dots and control the photoelectron motion. The proposed, designed, and investigated advanced QD structures have a set of characteristics making them especially suitable for IR: (i) Manageable photoelectron kinetics, which allows for tuning the photocarrier lifetime to control basic sensor characteristics, such as operating time, responsivity, and detectivity; (ii) Tunable highly-selective coupling to radiation due to control of QD levels; (iii) High photoconductive gain and responsivity; (iv) Low generation-recombination noise due to the long photoelectron lifetime. The research has produced a provisional patent, ten journal articles, seventeen conference presentations, and two Ph.D. dissertations. It was highlighted by SPIE Newsroom.

I. Approaches and Methods

The research focused on design and modeling of next generation quantum dot (QD) structures for IR detectors operating at room temperatures due to the large lifetimes of photocarriers. Carrier lifetime is a critical parameter for improving the efficiency of room-temperature semiconductor optoelectronic devices, such as mid- and far infrared detectors, solar cells, etc. [1-6]. For example, quantum-well infrared photodetectors (QWIPs) is currently a well-established technology, which is widely employed in various imaging devices working at liquid nitrogen temperatures and below [7,8]. At 77K, modern QWIPs operating around λ = 10 μm demonstrate the detectivity of ~10^{10} cmHz$^{1/2}$/W. The detectivity drops by two orders of magnitude as the temperature increases to the room temperature. It is well understood that the high-temperature limitations of QWIPs and many other photodetectors are caused by tremendous decrease of the photocarrier lifetime, which strongly reduces the detector's responsivity and sensitivity [1-4,7-10].

Quantum dot nanostructures were considered as a promising candidate for improving the room-temperature optoelectronic devices due to expected slow relaxation between discrete QD levels. These expectations were based on the "phonon bottleneck" concept, which assumes that the phonon-assisted bound-to-bound transitions are prohibited, unless the energy between two discrete levels matches to the phonon energy [11]. According to this concept, the intrinsic electron relaxation in quasi-1D nano-objects, such as QDs, was anticipated to be significantly slower than that in 2D and 3D structures. However, the phonon bottleneck model completely ignores modification of electron states due to interaction effects, e.g. due to a finite width of electron energy levels. It is not surprising that the experimentally measured phonon-mediated electron relaxation turned out to be much faster than it is expected in the phonon bottleneck concept [12-14]. Recent investigations [1] unambiguously demonstrated that the actual intra-dot kinetics is completely opposite to what can be expected for weakly interacting electrons and phonons [11]. In reality, strong coupling between electrons and longitudinal optical (LO) phonons leads to formation of the polaron states, which decay due to the interaction of LO phonons with acoustical phonons. Such kinetics results in strong energy and temperature dependences of the electron relaxation. At helium temperature, long relaxation time (~ 1.5 ns) was observed for the level separation of 14 meV (3.4 THz) [1]. However, the relaxation time decreases to ~ 2 ps for the 30 meV transition. The relaxation time also drastically decreases, if temperature increases. For example, for 14 meV transition, the relaxation time was measured to reduce from 1.5 ns at 10K to 560 ps at 30 K, and further to 260 ps at 50 K. At room temperatures the polaron decay time is observed in the range of 2 – 30 ps, depending on the electron energy [1]. Thus, after numerous experiments with various QD structures, no true phonon bottleneck has been found [1,2,12-14]. Thus, the intra-dot electron relaxation at room temperatures turns out to be very fast and practically unmanageable.

Recent advances in nanotechnology lead to new fascinating possibilities for controlling inter-dot kinetics of photoelectrons by means of potential barriers in specially engineered QD structures. In response to the challenges above and new technological opportunities, we propose and designed advanced QD structures.

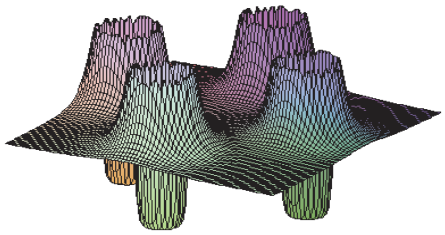

Fig. 1. *Potential barriers around single dots. The barriers are formed by electrons bounded in QDs and ionized dopants outside QDs.*

Our unique approach is based on engineering of photoelectron processes using (i) gate bias-manageable potential barriers around single QDs [15-18] and barriers around QD planes in the lateral structures [19-20] and (ii) barriers around QD clusters in the vertical structures [20-24].

Potential barriers around QDs are formed by electrons bounded in dots and ionized impurities in the depletion region. These potential barriers separate the conducting

electron states from the localized intra-dot states. Modern nanotechnologies provide various possibilities to fabricate QD structures with local and collective potential barriers. **Fig. 1** shows local potential barriers around single dots uniformly distributed in QD planes. Recently, in collaboration with E-Sensors, Inc. under AFOSR STTR program it was experimentally demonstrated that the potential barriers around single dots *exponentially* suppress the capture processes and in this way *exponentially* increase the photocarrier lifetime [18], which in turn increases the photoresponse (responsivity) and decrease the generation-recombination noise, i.e. improves the device sensitivity, in agreement with theoretical predictions.

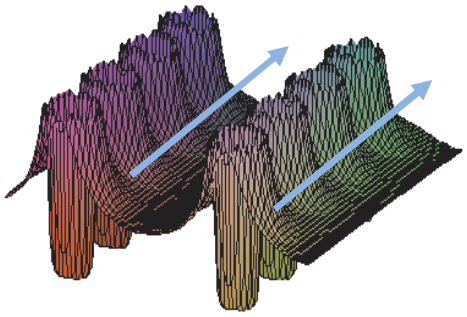

Fig. 2. *Collective potential barriers, created by QD rows with conducting channels between rows.*

To effectively suppress electron capture process, the barrier height should be at least two - three times larger than kT. Therefore, at room temperatures, the local barriers should be ~ 0.1 eV and, therefore, quantum dots should comprise ~ 5 - 10 electrons or more, which requires high level of doping. But even with relatively small doping, large potential barriers can be created around of groups of QDs (dot's clusters, rows etc). Such collective barriers divide these groups of QDs (for example, the dot rows in **Fig. 2**) from high-mobility conducting channels and drastically suppress the capture of photoelectrons. Changing the electron occupation of QDs by gate voltage, one can manage the potential barriers around dots and control the photoelectron lifetime and all related characteristics. We proposed advanced vertical and lateral QD structures with various collective potential barriers and investigated photoelectron kinetics in these structures.

To optimize the photodetector based on quantum-dot (QD) structures, a model of the room-temperature QD photodetector has been developed and investigated. Using analytical modeling and Monte-Carlo simulations, we have been stusied photoelectron kinetics, i.e. capture and transit processes, as functions of selective doping of a QD structure, its geometry, and electric field applied.

Monte-Carlo modeling is an effective tool for studying capture processes in external fields. Our simulation program includes all basic scattering processes, including electron scattering on acoustic, polar optical, and intervalley phonons. The modeling includes electrons in Γ-, L-, and X-valleys and takes into account redistribution of carriers between valleys. We simulate transport of three-dimensional electrons in GaAs matrix with InGaAs dots. We accept that the intradot relaxation processes are described by the relaxation time τ_ε', which is associated with the inelastic electron-phonon scattering in the dot area (see **Fig. 3 (b)**). Thus, here we consider the carrier capture process as a specific scattering process: (i) which is limited in space by the dot volume and (ii) in which a carrier transits from a

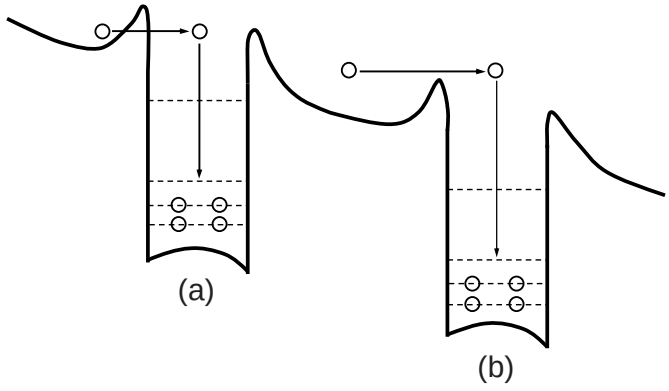

Fig. 3. *Photoelectron capture due to electron tunneling (a) and thermo-excitation (b).*

conducting state with the energy E_c above the potential barrier to a localized (bound) state E_l, which is below the potential barrier. In other words, we assume that from the bound state a carrier will relax to deeper dot states faster than it could return back to the conducting state. Using this model we investigate the dependence of the electron capture rate on the electric field at different values of the potential barrier, V_m.

II. Summary of Results

2.1 Photoelectron kinetics in structures with the single dot barriers

The only important assumption we accepted is that the probability of tunnelling processes is small compared with the capture probability via thermo-excitation above the potential barrier. Relative probability of tunneling and thermo-excitation capture processes can be evaluated taking into account the position of the turning point for electron tunneling [15]. Assuming that the barrier potential near the dot is close to the Coulomb potential, the position of the turning point, R_t, averaged over the thermal electron distribution is given by

$$R_t = a_B \left(\frac{Ry}{kT} \right)^{2/3} \left(Zm^* \right)^{1/3}, \tag{1}$$

where a_B is the Bohr radius, Ry is the Rydberg constant, Z is the charge of the dot, and m^* is the electron effective mass. In particular, for GaAs at room temperatures, R_t is about 4 nm. If the dot radius is larger than R_t the thermo-excitation will dominate over tunneling. Without tunneling processes, the photoelectron capture rate,

$$\tau_{capt}^{-1} = N_d \sigma \tilde{v}, \tag{2}$$

is given by the equation for the trapping cross-section,

$$\sigma = \pi \alpha a^2 \exp\left(-\frac{eV_m}{kT} \right) \left(1 + \frac{3}{4} \frac{\alpha a}{\ell} F(V) \right)^{-1}, \tag{3}$$

$$F = a \exp\left(-\frac{eV_m}{kT} \right) \int_a^b \frac{dr}{r^2} \exp\left(\frac{eV(r)}{kT} \right), \tag{4}$$

where $\tilde{v}$ is the electron thermal velocity, N_d is the concentration of quantum dots, a is the radius of the dot, b is the interdot distance, ℓ is the electron mean free path with respect to elastic electron scattering, α is the probability for an electron at $r \le a$ to be captured by the quantum dot, and V_m is the maximum value of the potential barrier, *i.e.* $V_m = V(a)$.

We would like to emphasize that Eqs. (3) and (4) are valid for any relation between ℓ, a, and αa as well as for wide variety of potential profiles. For example, for the flat potential profile $V = 0$, we get

$$\sigma = \pi \alpha a^2 \left[1 + \frac{3}{4} \frac{\alpha a}{\ell} \right]^{-1}.$$

(5) Describing the thermo-excitation processes, we accepted that the inelastic intradot relaxation processes are described by the relaxation time τ_ε'. In this case, the coefficient α can be evaluated

as $\alpha \approx a/\ell'_\varepsilon$, where $\ell'_\varepsilon = \tilde{\nu}'\tau'_\varepsilon$ and $\tilde{\nu}'$ is the electron thermal velocity in the dot. Then, if $a^2 << \ell\ell'_\varepsilon$, we obtain the capture rate:

$$\frac{1}{\tau_{capt}} = \pi N_d a^3 \frac{\tilde{\nu}}{\tilde{\nu}'} \frac{1}{\tau'_\varepsilon} \quad . \tag{6}$$

In the opposite case, $a^2 >> \ell\ell'_\varepsilon$, the capture rate is independent of the coefficient α and is given by

$$\frac{1}{\tau_{capt}} = 4\pi N_d D\, a \ , \tag{7}$$

where $D = \tilde{\nu}\ell/3$ is the diffusion coefficient.

We would like to note that the second term in the brackets in Eq. (3) describes the reduction of the carrier concentration near the dot. Due to the repulsive potential barriers this effect is increased by a factor of $F(V)$ given by Eq. (4). Comparing this result with the electron capture on repulsive impurity traps, one can associate $F(V)$ with the Sommerfeld factor, which shows the reduction of carrier density (electron wave function) near the trap. If local reduction of carrier density is negligible, then the capture rate is:

$$\frac{1}{\tau_{capt}} = \pi N_d\ a^3 \frac{\tilde{\nu}}{\tilde{\nu}'} \frac{1}{\tau'_\varepsilon} \exp\left(-\frac{eV_m}{kT}\right), \tag{8}$$

where the exponential factor describes the effect of potential barriers on capture processes.

Summarizing this subsection, we should note that, while the above formalism is general enough, however it is applicable only to quasi-equilibrium electron distributions, i.e. for low electric fields. At the same time, optimal regimes for operating of semiconductor detectors are always achieved in high electric fields, which generate nonequilibrium carrier distributions.

Employing the Monte-Carlo modelling we investigate the dependence of the electron capture rate on the

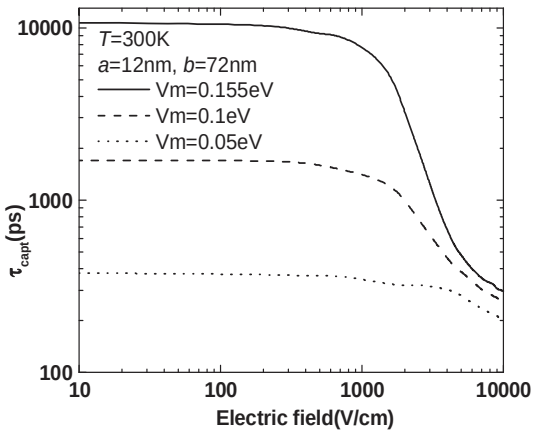

Fig. 4. *Capture time vs the electric field at various potential barriers.*

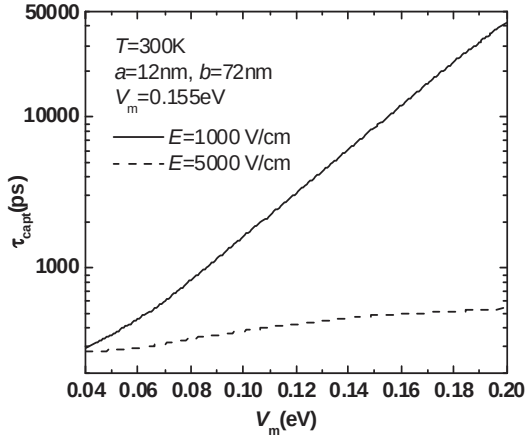

Fig. 5. *Capture time vs the barrier height.*

electric field at different values of the potential barrier, V_m. As seen in **Fig. 5**, the capture time is practically independent on the electric field up to the critical field F_c, which is of the order of 10^3 V/cm, and at fields higher than F_c it substantially decreases with the field increase. **Fig. 6** shows the dependence of the capture time on the magnitude of potential barrier, V_m. Note, that significant changes in this dependence appear only in electric fields higher than 1 kV/cm. While the absolute values of the capture rate depend strongly on intradot processes, the dependences of τ_{capt} on the electric field are modified just slightly in a wide range of variations of α. Thus, the characteristic value of the electric field F_c is mainly determined by the carrier transport in the matrix, and it is insensitive to the intradot processes.

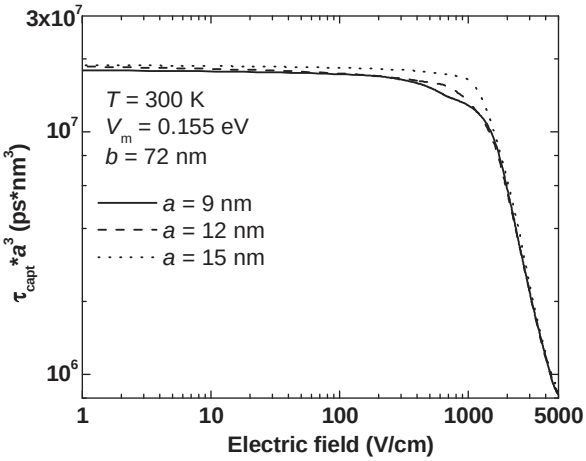

Fig.6. *Product of τ_{capt} and a^3 vs the electric field.*

To compare the data of our simulations with the analytical results, we investigated the dependence of the capture time, τ_{capt}, on the dot radius, a, in the electric field. As seen in **Fig. 6**, the product of τ_{capt} and a^3 is a universal function of the electric field F. Taking into account that at room temperature the electron mean free path ℓ is significantly larger than the dot radius, a, we expect that without electric field the capture rate is proportional to a^3, as it is described by Eq. (6). Our Monte-Carlo simulation results demonstrate that this is also valid in the presence of electric fields, including a wide range of high electric fields that substantially modify the capture rate.

In recent paper [25], it has been suggested that the conducting and localized electron states can be effectively separated in k-space as well as in real space. In particular, GaAs has a complex band structure, which consists of Γ-, L-, and X-valleys. In equilibrium electrons mainly populate Γ- valley. In high electric fields, electrons can transfer from Γ- to L- and X-valleys. The upper valleys are characterized by high values of electron masses and, therefore, by high densities of states. For this reason, in high electric fields the transfer to higher valleys is strongly enhanced. After electrons repopulate L- and X-valleys, the electron capture rate from these states into Γ-like localized states in the dots is substantially lower than that from Γ-valley, and therefore, the separation in the k-space may result in the significant reduction of the cross-section for capture processes.

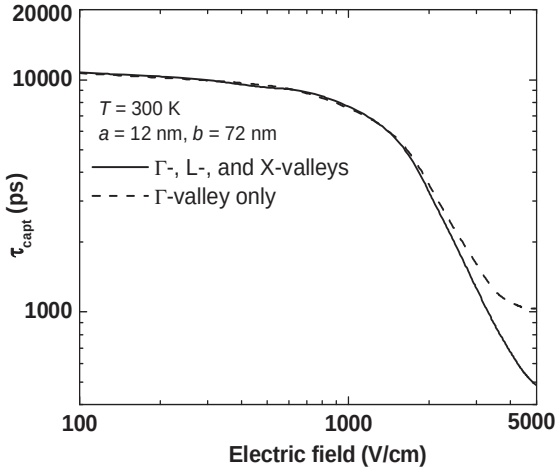

Fig. 7. *Capture time vs electric field: dashed line – without capture from higher valleys, solid line – capture from all valleys*

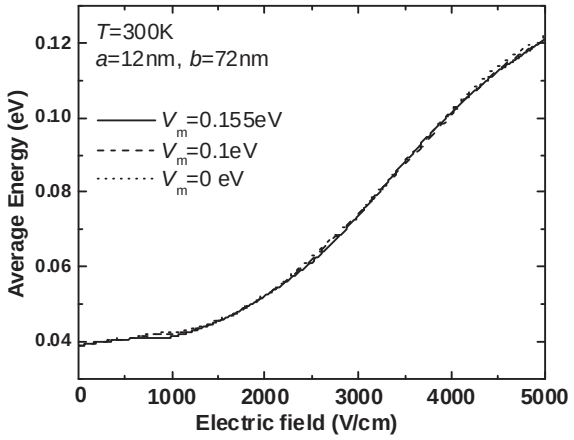

Fig. 8. *Average electron energy $\bar{\varepsilon}$ as a function of the electric field.*

To check this hypothesis, we calculated the capture time averaged over electrons in Γ-valley and compared it with the result for all electrons. As seen in **Fig. 7**, the effect of upper valleys in the carrier capture becomes important only at very high electric fields (~3 kV/cm), which are substantially larger than the characteristic fields F_c related to the potential barriers. Finally, let us try to analyze the modeling data in terms of electron heating. The dependence of the average electron energy $\bar{\varepsilon}$ on the electric field F is shown in **Fig. 8**. As expected, the potential barriers do not change the average energy of the electron gained in the electric field. In **Fig. 9**, we present the exponential dependence of the capture time on the inverse value of $\bar{\varepsilon}$. As seen, for two different potential barriers log τ_{capt} is proportional to $1/\bar{\varepsilon}$, i.e. we find that τ_{capt} is proportional to exp $(1/\bar{\varepsilon})$. Therefore, we may conclude that the carrier capture in the electric field can be described by Eq. (14), where the thermal energy kT can be replaced by a factor of $\sim 2\bar{\varepsilon}/3$. Thus, the carrier capture is well described by the model of electron heating.

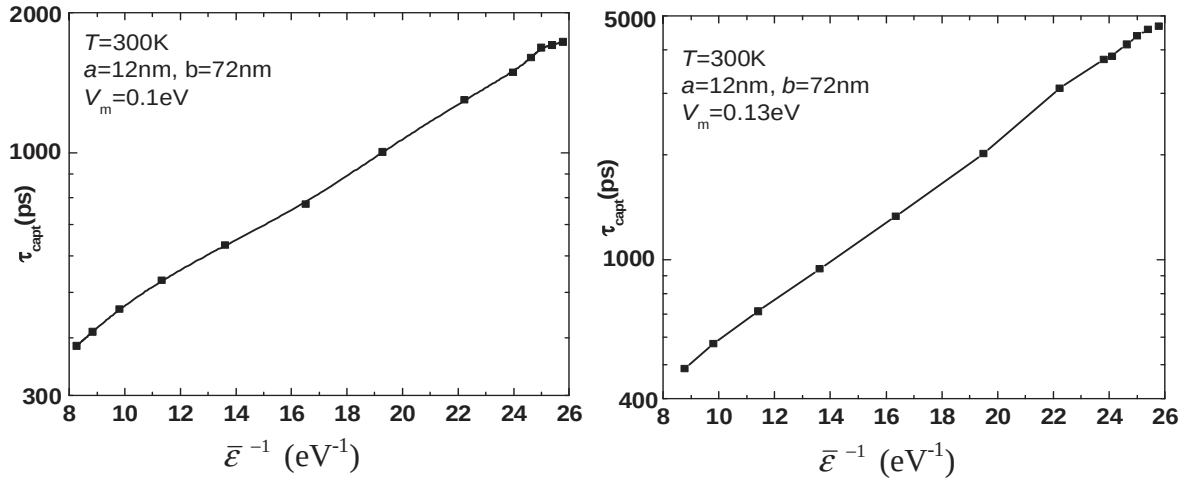

Fig. 9. *The capture time vs inverse electron energy attained in the electric field.*

In **Fig. 10** we present the photoconductive gain as a function of the electric field for a device with length of 1 μm. The average drift velocities have been calculated using the same Monte Carlo program that was employed to find the field dependence of the electron capture time. As it is seen, the gain reaches maximum value at electric field of ~1-5 kV/cm, which is also the characteristic field for the dependences shown in previous figures. This nonmonotonic dependence has a simple explanation. At low electric fields, where capture time, τ_{capt}, is almost constant, the gain increases due to a decrease of the transit time, τ_{tr}. At high electric fields, the gain decreases due to the exponential decrease of the capture time.

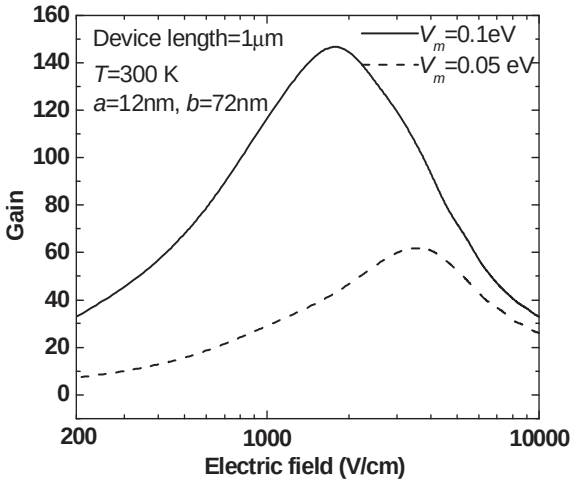

Fig. 10. *Gain vs of the electric field.*

Thus, results of our simulations demonstrate that the photoelectron capture is substantially enhanced in strong electric fields. Detailed analysis shows that effects of the electric field on electron capture in the structures with barriers are not sensitive to the redistribution of electrons between valleys. The data obtained find an adequate explanation in the model of hot-electron transport in the potential relief of quantum dots. We also demonstrated that the photoelectron kinetics is very sensitive to potential barriers of intentionally or unintentionally charged quantum dots. The capture processes can be substantially suppressed by a proper choice of the geometry of a QD structure and modulation doping. The developed model is in agreement with the available experimental results [25].

2.2. Photoelectron kinetics in QD structures with the lateral transport

First, let us present our results for ordinary QD structures with evenly distributed QDs in QD planes, but with the lateral transport of photocarriers along QD planes. Such devices may be fabricated on the base of the modulation-doped AlGaAs/GaAs with self-assembled InAs QDs (see **Fig. 11**). QD layers are imbedded in the middle of GaAs quantum wells with a thickness of 2*d*. AlGaAs layers are doped to supply the dots with electrons or holes. Ohmic contacts to the lateral QD structures may be fabricated by depositing and annealing AuNiGe alloy. Because of the complex contact technology to the lateral structures, the interelectrode distance in available devices is relatively large, of the order of 100 μm.

The band diagram of the structure is shown in **Fig. 11.b**. Potential barriers are created by the charged QD planes and charged planes of dopants. Photoexcited carriers move along areas with high mobility near the modulation-doped heterointerfaces. Thus, potential barriers between high-mobility conducting states and localized states in QDs are proportional to the distance between the QD plane and AlGaAs layer, i.e. to *d*.

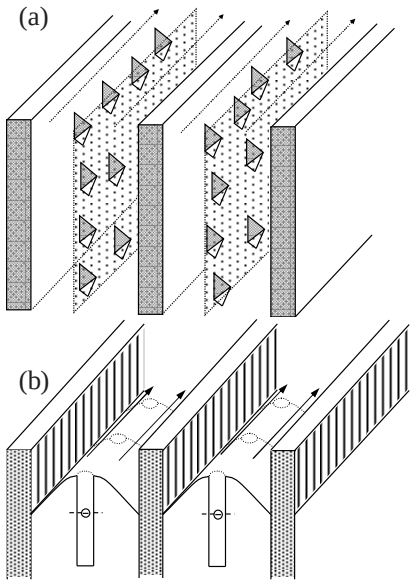

Fig. 11. *The QDIP with the lateral transport (a) and the corresponding band structure*

Our results show that in small electric fields, the capture time exponentially increases with increasing of the height of the potential barrier V_m. In the lateral structures, the potential is created by charged planes and may be presented as $V_m = e^2 N_d^{(2)} nd/(2\varepsilon\varepsilon_0)$ (see the insert in **Fig. 12**), where $N_d^{(2)}$ is the dot concentration in QD planes, and n is the occupation, i.e. an average number of carriers per dot. Thus, the capture time exponentially increases with increasing of the dot concentration, occupation, and the well width d. In **Fig. 12** we present the dependence of the capture time on the occupation n for typical parameters: $N_d^{(2)} = 0.4 \cdot 10^{11}$ cm^{-2} and d = 80 nm. As for QD structures with local barriers, the effect of the electric field can be understood in terms of the electron heating. The electric field increases the average energy (temperature) of carriers, so the barriers are less effective in preventing capture of hot electrons. Therefore, the capture time decreases as the electric field increases. The detector responsivity is proportional to the photoconductive gain g_{ph}, which is defined as

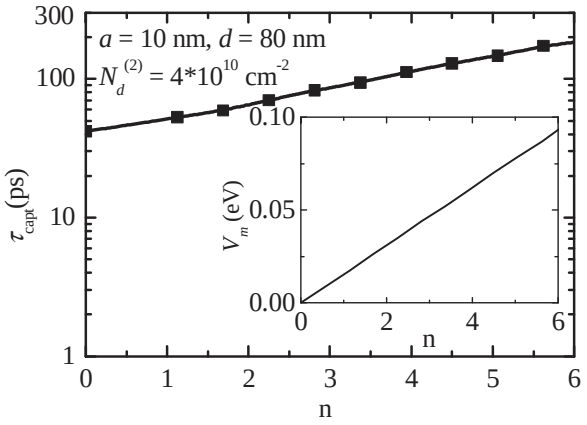

Fig. 12. *Capture time and the barrier height (insert) vs the occupation n.*

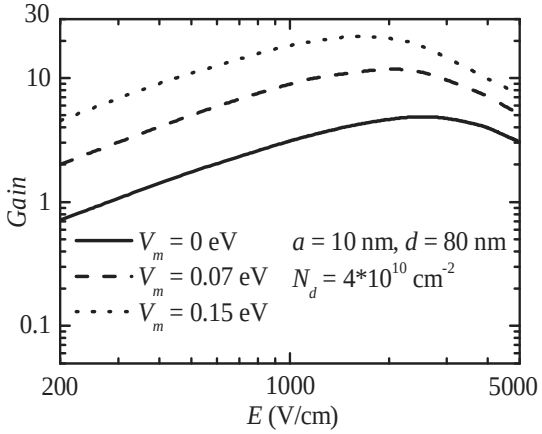

Fig. 13. *Photoconductive gain as a function of the electric field.*

a ratio of the photoelectron lifetime τ_ℓ to the transit time $\tau_{tr}=L/\mu E$. In **Fig. 13** we show the dependence of the gain on the electric field. The initial increase of g_{ph} is due to the decrease of the transit time. The decrease of g_{ph} in strong fields is due to a decrease of the capture time. Our modeling demonstrates that collective barriers significantly increase the photoelectron lifetime and photoconductive gain in lateral QD structures at room-temperatures.

The photoelectron kinetics in the lateral structures was experimentally investigated only at liquid nitrogen temperatures. It was found that the photocarrier lifetime and the detector responsivity depend exponentially on *d*. The lifetime was determined to be as long as 3 ms. The corresponding photoconductive gain was evaluated as ~10^6. In this way a critical role of the collective potential barriers in lateral structures was fully confirmed by measurements at T=77K [26]. Our simulations demonstrated a strong potential of these structures for room temperature operation and encourage experimentalists to start fabrication of corresponding devices.

2.3 Photoelectron kinetics in structures with vertically correlated dot clusters

Advantages of QWIPs with the vertical transport over the lateral QWIPs include a short intercontact distance and the well-established processing technologies, which provide high-quality reproducible Ohmic contacts. The short detector base decreases the generation-recombination noise and increases the photoconductive gain. The high-quality Ohmic contacts are also important for noise characteristics. To combine the advantages of the vertical QDIPs with the concept of barrier-limited capture, we propose the detectors based on structures with vertically correlated dot clusters (VCDC).

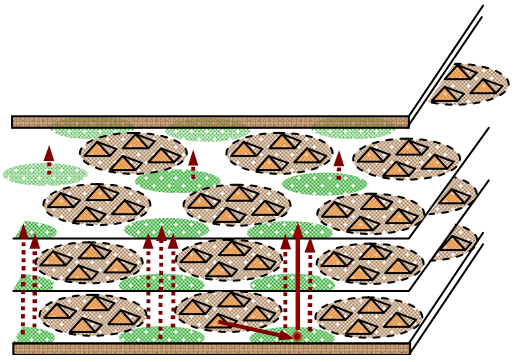

Fig. 14. *Nanostructure with vertically correlated dot clusters (VCDC), where the photoelectron transport (red arrows) is separated from QDs by potential barriers.*

In the VCDC structures presented in **Fig. 14** the positions of quantum dot clusters in each layer are correlated in the vertical direction, i.e. in the direction of photocurrent. The collective barriers around the dot clusters are formed by the carriers in the dots. The barriers separate the conducting channels in the matrix and the localized electron states in quantum dots and therefore could suppress the electron capture into dots. Once the electrons are excited by the radiation, electrons

drift in the areas between dot clusters through high-mobility conducting channels, as shown by the red arrows in **Fig. 14**. Compared to the QD structures with the lateral transport shown in **Fig. 11**, the conducting channels of VCDC structures has a cylindrical form, as it is shown in **Fig. 15**. If the radius of the cluster, *b*, exceeds the distance between dot planes, *c*, the potential barrier around clusters has a logarithmic form $V_m = e^2Nn/(2\pi\varepsilon\varepsilon_0 c)\ln(w/b)$, where *N* is the number of QDs in the cluster, *n* is the average occupation in the dot, and 2*w* is the distance between the centres of the nearest two clusters.

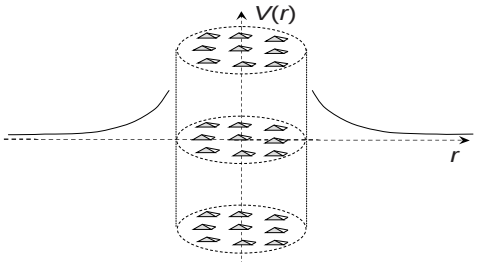

Fig. 15. *Logarithmic potential barriers around vertically correlated dot clusters.*

Below we present results of our modelling for $N = 9$, $b = 75$, and $c = 40$. The distance between the dots is 55 nm. Since the barrier height is determined by the dot concentration and dot occupation, the capture time exponentially increases with these factors. Besides, the capture processes are weakly sensitive to geometrical parameters *w* and *b* due to the logarithmic form of potential. **Fig. 16** illustrates the exponential dependence of the capture time on the dot occupation. This dependence is explained by the linear dependence of potential barrier height on the dot occupation (**Fig. 17**) and by the exponential dependence of capture time on the potential barrier height. Since potential barrier has a logarithmic dependence on *w*, the photoelectron capture time weakly depends on this geometrical parameter.

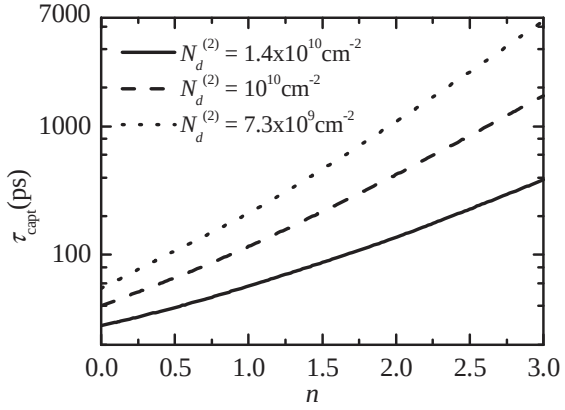

Fig. 16. *Capture time vs dot occupation.*

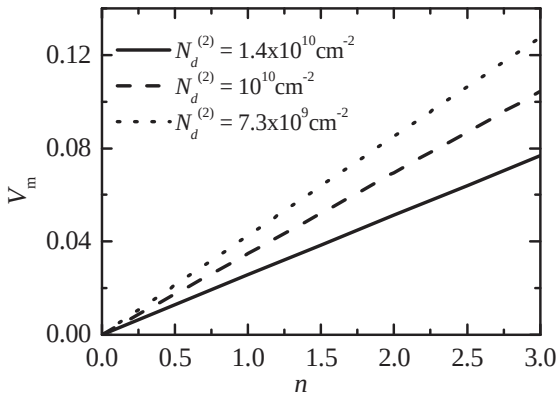

Fig. 17. *Barrier height vs dot occupation.*

Fig. 18 shows the dependence of capture time on dot concentration. Modern fabrication technologies can produce QDIPs with dot concentration ~10^9 – 10^{11} dots/cm^2. At fixed occupation, *n*, the potential barrier height increases slightly with the decreasing of dot concentration due to logarithmic dependence on *w*. Therefore, the capture time decreases with increase of the dot concentration, as it is shown in **Fig. 18**.

Fig. 19 presents the capture time as a function of electric field for three values of occupation. In order to contribute to the photocurrent, photo-excited carriers are driven by the applied bias. At small electric field, photocarriers are accelerated and the drift velocity linearly increases. When the electric field reaches a characteristic value, which is of the order of 10^3 V/cm, the electric field effectively heats the electrons. Electron heating increases an average energy of photoelectrons, which allows them to overcome potential barriers. Therefore, in the electric fields above ~10^3 V/cm the capture time decreases dramatically.

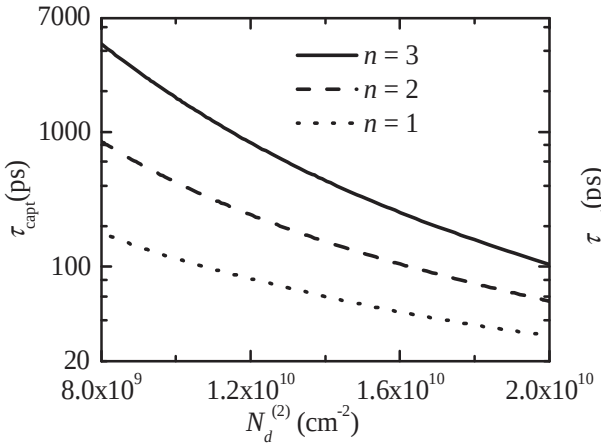

Fig. 18. *Capture time vs. dot concentration.*

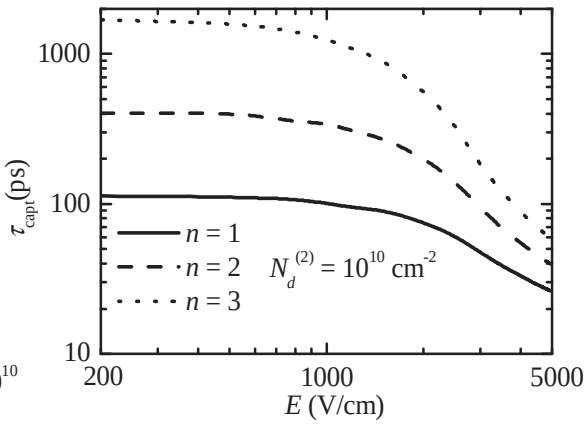

Fig. 19. *Capture time vs. electric field.*

Fig. 20 shows the average electron energy as a function of the electric field, as it was found from the Monte-Carlo modelling. Let us note that the average electron energy may also be evaluated from the energy balance equation, if one assumes that the nonequilibrium electron distribution function is described by electron temperature. Both numerical and analytical calculations provide consistent results. **Fig. 21** shows the dependence of the capture time on the inverse of average electron energy. The result demonstrates that the capture time is proportional to $\exp(1/\bar{\varepsilon})$. Thus, the carrier capture in the electric field can be described by our analytical model developed for small electric fields, if the thermal energy kT

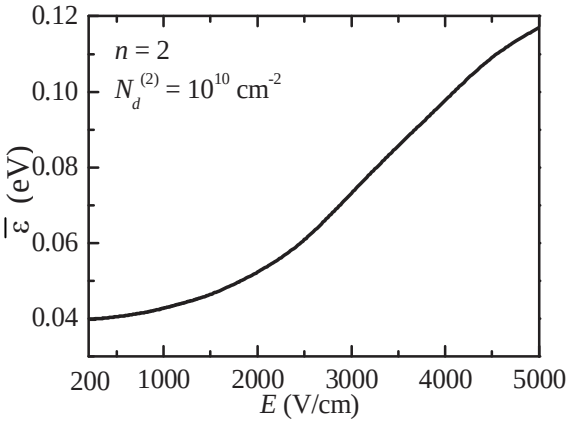

Fig. 20. Average electron energy vs. electric field.

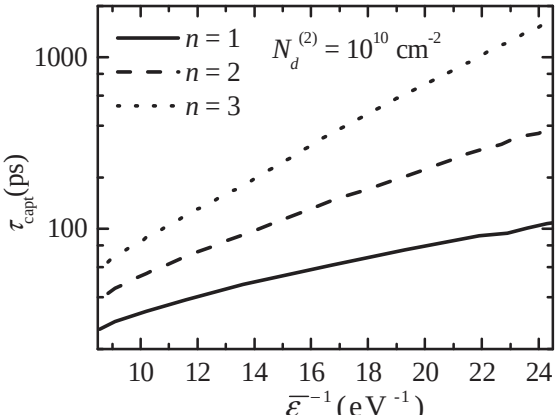

Fig. 21. Capture time vs. inverse electron energy.

is replaced by a factor of $\sim 2\bar{\varepsilon}/3$. Thus, we may conclude that the effect of the electric field on carrier capture is well described by the model of electron heating.

In **Fig. 22** we present the photoconductive gain, g, as a function of the electric field for a device with the length of 1 μm. Photoconductive gain is defined as the ratio of the carrier lifetime, τ_{cap}, to carrier transit time, τ_{tr}. Transit time is the time that the electron spends in the device moving from the emitter to the collector and, therefore it is inversely proportional to the drift velocity. The average drift velocities have been calculated using the same Monte Carlo program that was employed to find the field dependence of the electron capture time. As seen in the **Fig. 22**, the gain approaches a maximum value at electric field of the order of 10^3 V/cm, which is also the characteristic field for the dependences shown in **Fig. 19**. This nonmonotonic dependence on the electric field may be explained in the following way. At small electric fields, the gain increases with increasing of the electric field, since the transit time reduces and capture time remains almost constant. When the electric field increases up to a characteristic value, transit time almost saturates and capture time is substantially reduced and, therefore, the gain decreases substantially.

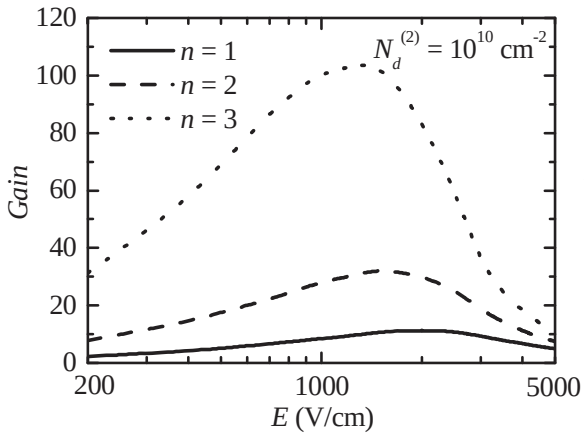

Fig. 22. Gain vs. electric field.

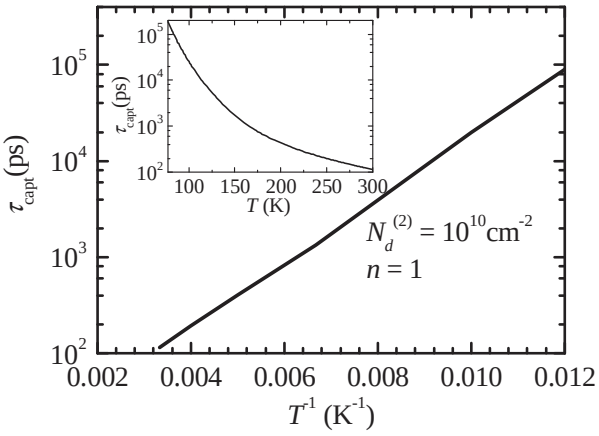

Fig. 23. Capture time vs. 1/T and T (insert).

Finally, **Fig. 23** shows the dependence of the capture time on the temperature at fixed potential barrier. We can see that the capture time is proportional to $\exp(1/kT)$. Let us highlight it again that at all temperatures the barriers effectively suppress the capture processes.

2.4 Experimental confirmation of the effect of potential barriers on photoelectron kinetics

To directly investigate effects of potential barriers on photoresponse, several QD structures with various positions of dopants and various levels of doping were fabricated. The first set of nanostructure has been grown with Si doping during the InAs dot growth. The second set has been grown with the Si Delta doping directly in the middle of each AlGaAs barrier layer. The third set has been grown with the modulation doping. The level of doping changes significantly, from $2.7 \cdot 10^{11}$ cm^{-2} to $8 \cdot 10^{11}$ cm^{-2}. It has been observed that the photoresponse exponentially increases when the potential barriers. Thus, in our measurements the photoresponse increases by ~ 30 times as the dot population increases up to nine electrons per dot [18].

References

1. E. A. Zibik, T. Grange, B. A. Carpenter, N. E. Porter, R. Ferreira, G. Bastard, D. Stehr, S. Winnerl, M. Helm, H. Y. Liu, M. S. Skolnick, and L. R. Wilson, “Long lifetimes of quantum-dot intersublevel transitions in the terahertz range,” *Nature Materials* **8**, 403 (2009).
2. M. Razeghi, H. Lim, S. Tsao, J. Szafraniec, W. Zhang, K. Mi, and B. Movaghar, “Transport and photodetection in self-assembled semiconductor quantum dots,” *Nanotechnology* **16**, 219 (2005).
3. J. C. Campbell and A. Madhukar, "Quantum Dot Infrared Detectors," *IEEE Quantum Electronics* **95**, 1815 (2007).
4. A.V. Barve, S.J. Lee, S.K. Noh, S. Krishna, “Review of current progress in quantum dot infrared photodetectors,” *Laser & Photonics Reviews*, June 17, (2009).
5. M.D. Kelzenberg, D.B. Turner-Evans, B.M. Kayes, M.A. Filler, M.C. Putnam, N.S. Lewis, H.A. Atwater et al., “Photovoltaic measurements in single-nanowire silicon solar cells,” *NANO Letters* **8**, 710 (2008).
6. H. Spanggaard, F.C. Krebs, “A brief history of the development of organic and polymeric photovoltaics,” *Solar Energy Materials and Solar Cells* **83**, 125 (2004).
7. B. F. Levine, “Quantum-well infrared photodetectors,” *J. Appl. Phys*. **74** R1 (1993).

8. S.D. Gunapala, S.V. Bandara, J.K. Liu, C.J. Hill, S.B. Rafol, J.M. Mumolo, J.T. Trinh, M.Z. Tidrow and P.D. LeVan, "1024 × 1024 pixel mid-wavelength and long-wavelength infrared QWIP focal plane arrays for imaging applications," *Semicond. Sci. Technol.* **20,** 473 (2005).
9. P. Bhattacharya, X. H. Su, S. Chakrabarti, G. Ariyawansa, and A. G. U. Perera, "Characteristics of a tunneling quantum-dot infrared photodetector operating at room temperature," *Appl. Phys. Lett.* **86**, 191106 (2005).
10. S. Tsao, H. Lim, W. Zhang, and M. Razeghi, "High operating temperature 320×256 middle-wavelength infrared focal plane array imaging based on an InAs/InGaAs/InAlAs/InP quantum dot infrared photodetector," *Appl. Phys. Lett.* **90**, 201109 (2007).
11. U. Bockelmann and G. Bastard, "Phonon scattering and energy relaxation in two-, one-, and zero-dimensional electron gases," *Phys. Rev. B* **42**, 8947 (1990).
12. Y. Toda, O. Moriwaki, M. Nishioka, and Y. Arakawa, "Efficient carrier relaxation mechanism in InGaAs/GaAs self-assembled quantum dots based on the existence of continuum states," *Phys. Rev. Lett.* **82**, 4114 (1999).
13. R. Ferreira and G. Bastard, "Phonon-assisted capture and intradot Auger relaxation in quantum dots," *Appl. Phys. Lett.* **74**, 2818 (1999).
14. H. Lim, B. Movaghar, S. Tsao, M. Taguchi, W. Zhang, A. A. Quivy, and M. Razeghi, "Gain and recombination dynamics of quantum-dot infrared photodetectors," *Phys. Rev. B* **74**, 205321 (2006).
15. A. Sergeev, V. Mitin, and M. Stroscio, "Quantum-dot photodetector operating at room temperatures: diffusion-limited capture," *Physica B* **316-317**, 369 (2002).
16. V. Mitin, A. Sergeev, L.-H. Chien, and N. Vagidov, "High performance of IR detectors due to controllable kinetics in quantum-dot structures," *Proc. SPIE* **7095**, 70950K (2008).
17. L.H. Chien, A. Sergeev, N. Vagidov, and V. Mitin, "Hot-electron transport in quantum-dot photodetectors, series "Selected Topics in Electronics and Systems," Vol. 50, World Scientific, New Jersey, pp.255-264 (2009).
18. V. Mitin, A. Antipov, A. Sergeev, N. Vagidov, D. Eason, and G. Strasser, "Quantum dot infrared photodetectors: Photoresponse enhancement due to potential barriers," *Nanoscale Reserach Letters*, excepted, available at *NANO EXPRESS, on line first* (2010).
19. L.-H. Chien, A. Sergeev, V. Mitin, and S. Oktyabrsky, "Quantum dot photodetectors based on structures with collective potential barriers," *Proc. SPIE* **7608**, 760826 (2010).
20. V. Mitin, A. Sergeev, L-H. Chien, and N. Vagidov, "Monte-Carlo modeling of electron kinetics in room temperature quantum-dot photodetectors," in *Large-Scale Scientific Computing*, eds. I. Lirkov and S. Margenov, Spinger Berlin / Heidelberg, 2010, pp. 403-410.
21. L.-H. Chien, A. Sergeev, V. Mitin, N. Vagidov, and S. Oktyabrsky, "Nanostructures with quantum dot clusters," Long photocarrier lifetime, *Nanoscience and Nanotechnology Letters* **2**, 1 (2010).
22. V. Mitin, A. Sergeev, L.-H. Chien, A. Antipov, and G. Strasser, "Photodetectors on structures with vertically correlated dot clusters," *Proc. SPIE* **7679**, 767905 (2010).
23. A. Sergeev, V. Mitin, and G. Strasser, "Nanostructures for long photoelectron lifetime," *SPIE Newsroom*, 29 March 2010, http://spie.org/x39405.xml?highlight=x2400&ArticleID=x3940.
24. A. Sergeev, L-H. Chien, N. Vagidov, and V. Mitin, "Quantum-dot infrared photodetectors: In search of right design for room-temperature operation," in *Future Trends in Microelectronics: From Nanophotonics to Sensors to Energy*, editors S. Luryi, J. Xu, and A. Zaslavsky, Wiley-IEEE Press, 2010, p. 385.

25. Matthews, M.R., Steed, R.J., Frogley, M.D., Phillips, Ch.C., Attaluri, R.S., and Krishna, S., "Transient photoconductivity measurements of carrier lifetimes in an InAs/In0.15Ga0.85As dots-in-a-well detector," Appl. Phys. Lett. 90, 103519 (2007).
26. K. Hirakawa, S.-W. Lee, Ph. Lelong et al., "High-sensitivity modulation-doped quantum dot infrared photodetectors," *Microelectronic Engineering* **63**, 185 (2002).

III. Personnel Supported by this grant

Graduate Students:
LiHsin Chien
Andrey Antipov

Researchers
Assistant Research Professor Nizami Vagidov
Associate Research Professor Andrei Sergeyev (Co-I)
Professor Vladimir Mitin (PI)

IV. Patent disclosures

1. "***Structures with Vertically Correlated Quantum-Dot Clusters for Detector and Solar Cell Applications***," A. Sergeev, G. Strasser, and V. Mitin, Provisional Patent R-6446.

V. Articles

1. "Infrared Quantum-Dot Photodetectors with Diffusion-Limited Capture," N. Vagidov, A. Sergeev, and V. Mitin, in *Physics and Modeling of Tera- and Nano-Devices*, editors M. Ryzhii and V. Ryzhii, World Scientific, pp. 141-148, 2008.
2. "High Performance of IR Detectors due to Controllable Kinetics in Quantum-Dot Structures," V. Mitin, A. Sergeev, L. Chen, and N. Vagidov, *Proceed. of SPIE*: Nanophotonics and Macrophotonics for Space Environment II, Vol 7095, pp. 70950K-1-9, 2008.
3. a. "Hot-Electron transport in quantum-dot photodetectors", L. Chien, A. Sergeev, N. Vagidov, V. Mitin, *Int. J. High Speed Electron. Syst*. (IJHSES) Vol.18, No.4, pp.1013-1022 (2008);

   b. "Hot-Electron transport in quantum-dot photodetectors", L. Chien, A. Sergeev, N. Vagidov, V. Mitin, "Frontiers in Electronics", Eds. S. Cristoloveanu and M.S. Shur, series "*Selected Topics in Electronics and Systems*", Vol. 50, World Scientific, New Jersey, pp.255-264 (2009).
4. "Graphene nanoribbon phototransistor: proposal and analysis", V. Ryzhii, M. Ryzhii, N. Ryabova, V. Mitin, and T. Otsuji. Jpn. J. Appl. Phys. 48, pp. 04C144 (2009).
5. "Monte-Carlo modeling of electron kinetics in room temperature quantum-dot photodetectors," V. Mitin, A. Sergeev, L-H. Chien, and N. Vagidov, in *Large-Scale Scientific Computing*, eds. I. Lirkov and S. Margenov, Spinger Berlin / Heidelberg, 2010, pp. 403-410.
6. "Quantum-Dot Infrared Photodetectors: In Search of Right Design for Room-Temperature Operation," A. Sergeev, L-H. Chien, N. Vagidov N., and V. Mitin, in *Future Trends in Microelectronics: From Nanophotonics to Sensors to Energy*, editors S. Luryi, J. Xu, and A. Zaslavsky, Wiley-IEEE Press, 2010, p. 385.
7. "Quantum dot photodetectors based on structures with collective potential barriers," L-H. Chien, A. Sergeev, V. Mitin, and. S. Oktyabrsky, *Proc. SPIE* **7608**, 760826 (2010).
8. "Photodetectors on structures with vertically correlated dot clusters," V. Mitin, A. Sergeev, L.-H. Chien, A. Antipov, and G. Strasser: *Proc. SPIE* **7679**, 767905 (2010).

9. "Nanostructures with quantum dot clusters: Long photocarrier lifetime," L.-H. Chien, A. Sergeev, V. Mitin, N. Vagidov, and S. Oktyabrsky: *Nanoscience and Nanotechnology Letters* **2**, 1 (2010).
10. "Quantum Dot Infrared Photodetectors: Photoresponse Enhancement due to Potential Barriers," V. Mitin, A. Antipov, A. Sergeev, N. Vagidov, D. Eason, and G. Strasser: *Nanoscale Research Letters*, accepted; available at *"online first"* NANO EXPRESS (2010).

Dissertations

1. Andrey Antipov, ***"Quantum Dots: Structures, Properties, and Applications,"*** The State University of New York at Buffalo, Department of Electrical Engineering, 2010.
2. LiHsin Chien, "***Quantum Dot Infrared Photodetectors Based on Structures with Potential Barriers: Modeling and Optimization,"*** The State University of New York at Buffalo, Department of Electrical Engineering, 2010.

Web Presentations

1. "Nanostructures for long photoelectron lifetime," A. Sergeev, V. Mitin, and G. Strasser: *SPIE Newsroom*, 29 March 2010, DOI: 10.1117/2.1201002.002625, http://spie.org/x39405.xml?highlight=x2400&ArticleID=x39405

Conference Presentations

1. "Quantum-Dot Photodetectors: High Sensitivity due to Controllable Kinetics", A. Sergeev, L. Chien, N. Vagidov, and V. Mitin, American Physical Society Meeting, March 10-14, 2008, New Orleans, LA, Program, p. R1.00106.
2. "High Performance of IR Detectors due to Controllable Kinetics in Quantum-Dot Structures," V. Mitin, A. Sergeev, L. Chen, and N. Vagidov, SPIE Optics + Photonics 2008 Symposium, August 10-14, 2008, San Diego, CA.
3. "High Performance of Room-Temperature IR Detectors due to Controllable Kinetics in Quantum-Dot Structures," Mitin, A. Sergeev, L. Chen, and N. Vagidov, 13th Advanced Heterostructures and Nanostructures Workshop, December 7-12, 2008, Hawaii.
4. "Device Models for Graphene Nanoribbon and Graphene Bilayer Phototransistors", V. Mitin, M. Ryzhii, T. Otsuji, N. Kirova, and V. Ryzhii, International Symposium on Graphene Devices: Technology, Physics and Modeling, November 17-19, 2008, Aizu-Wakamatsu, Japan, Technical Digest, pp 46-48.
5. "Some Concepts of Graphene-Based Electron and Optoelectron Devices", V. Ryzhii, M. Ryzhii, A. Satou, N. Ryabova, V. Mitin, and T. Otsuji, 13th Advanced Heterostructures and Nanostructures Workshop, December 7-12, 2008, Hawaii, program, p. 7.
6. "Graphene-based terahertz lasers and detectors: Physics and feasibility of realization", M. Ryzhii, A. Satou, V. Ryzhii, V. Mitin, F. T. Vasko, V. Ya. Aleshkin, A. A. Dubinov, and T. Otsuji, ESF-FWF Conf. Graphene Week 2009, March 2-7, 2009. Obergurgl, Austria.
7. "Design and operating regimes of quantum-dot photodetectors for room temperature operation," L. Chen, A. Sergeev, V. Mitin, 2009 APS March Meeting, March 16-20, 2009, Pittsburgh, PA, Poster Session C1
8. "Monte-Carlo modeling of photoelectron kinetics in quantum-dot photodetectors," V. Mitin, A. Sergeev, L-H. Chien, and N. Vagidov, 13th International Workshop on Computational Electronics, May 27-29, 2009, Beijing, China, pp. 219 - 222.

9. “Monte-Carlo modeling of electron kinetics in room temperature quantum-dot photodetectors,” V. Mitin, A. Sergeev, L-H. Chien, and N. Vagidov, 7th International Conference on “Large-Scale Scientific Computations”, June 4-8, 2009, Sozopol, Bulgaria, pp. 77 - 78.

10. “Quantum-dot photodetectors: In search of optimal design for room-temperature operation,” V. Mitin, L. Chien, N. Vagidov, and A. Sergeev, 2009 Advanced Research Workshop “Future Trends in Microelectronics: Unmapped Roads”, June 14-19, 2009, Sardinia, Italy, p. 54.

11. "Graphene nanoribbon and graphene bilayer photodetectors: models and characteristics," M. Ryzhii, V. Ryzhii, T. Otsuji, and V. Mitin, 14th Int. Conf. on Narrow Gap Semiconductors and Systems, July 13-17, 2009, Sendai, Japan, book of abstracts.

12. “Room temperature quantum-dot photodetectors: structures with collective potential barriers,” G. Strasser, A. Antipov, A. Sergeev L. Chien, N. Vagidov, and V. Mitin, ITQW 2009: 10th International Conference on Intersubband Transitions in Quantum Wells, September 6-11, 2009 Montreal, Canada, p.2.

13. “Quantum dot photodetectors based on structures with collective potential barriers,” A. Antipov, G. Strasser, A. Sergeev, L.H. Chien, N. Vagidov, V. Mitin, SPIE Photonics West 2010, January 23-28, 2010, San Francisco, CA, 7608-73.

14. “Quantum-Dot Infrared Photodetectors: Strutures with Correlated Dot Clusters for Room Temperature Operation,” V. Mitin, A. Antipov, L.H. Chien, A. Sergeev, G. Strasser, N. Vagidov, S. Birner, 16th International Winterschool Mauterndorf , February 22-26, Mauterndorf, Austria, book of abstracts, p. 198.

15. “Quantum dot photodetectors: Structures with collective potential barriers,” A. Sergeev, L.H. Chien, V. Mitin, S. Oktyabrsky, 2010 APS March Meeting, March 15-19, 2010, Portland, OR, Poster Session S1

16. “Photodetectors on sturtures with vertically correlated dot clusters,” V. Mitin, A. Sergeev, L.H. Chien, A. Antipov, G. Strasser, Invited Talk: SPIE Defense, Security and Sensing 2010, April 5-9, 2010, Orlando, FL, 7679-04.

17. “Quantum Dot Infrared Photodetectors: Structures with Vertically Correlated Dot Clusters,” V. Mitin, A. Sergeev, N. Vagidov, G. Strasser, A. Antipov, and L-H. Chien, Invited: 2010 Villa Conference on Interaction among Nanostructures (VCIAN), June 21-25, 2010, Santorini, Greece, book of abstracts, page 15.